Single-Photon-Resolved Cross-Kerr Interaction for Autonomous Stabilization of Photon-Number States

E. T. Holland,[1] B. Vlastakis,[1] R. W. Heeres,[1] M. J. Reagor,[1] U. Vool,[1] Z. Leghtas,[1] L. Frunzio,[1] G. Kirchmair,[1,2,3] M. H. Devoret,[1] M. Mirrahimi,[1,4] and R. J. Schoelkopf[1]

[1]*Departments of Physics and Applied Physics, Yale University, New Haven, Connecticut 06520, USA*
[2]*Institute for Quantum Optics and Quantum Information of the Austrian Academy of Sciences, A-6020 Innsbruck, Austria*
[3]*Institute for Experimental Physics, University of Innsbruck, A-6020 Innsbruck, Austria*
[4]*INRIA Paris-Rocquencourt, Domaine de Voluceau, B.P. 105, 78153 Le Chesnay Cedex, France*

(Received 13 April 2015; revised manuscript received 23 July 2015; published 26 October 2015)

Quantum states can be stabilized in the presence of intrinsic and environmental losses by either applying an active feedback condition on an ancillary system or through reservoir engineering. Reservoir engineering maintains a desired quantum state through a combination of drives and designed entropy evacuation. We propose and implement a quantum-reservoir engineering protocol that stabilizes Fock states in a microwave cavity. This protocol is realized with a circuit quantum electrodynamics platform where a Josephson junction provides direct, nonlinear coupling between two superconducting waveguide cavities. The nonlinear coupling results in a single-photon-resolved cross-Kerr effect between the two cavities enabling a photon-number-dependent coupling to a lossy environment. The quantum state of the microwave cavity is discussed in terms of a net polarization and is analyzed by a measurement of its steady state Wigner function.

DOI: 10.1103/PhysRevLett.115.180501 PACS numbers: 03.67.Pp, 03.65.Yz, 42.50.Dv, 85.25.-j

Decoherence is an unavoidable adversary in quantum information science. A large-scale quantum computer must implement error correction protocols to protect quantum states from decoherence [1]. A first step toward fault tolerant quantum error correction is the stabilization of a particular quantum state in the presence of decoherence [2]. One such implementation uses gate-based architectures with measurement and feedback [3–14] for the correction of quantum errors. An alternative approach to active quantum systems is quantum-reservoir engineering (QRE) [15–18], which harnesses persistent, intentional coupling to the environment as a resource. Both cases require entropy removal, yet only QRE employs environmental losses as a crucial part of their protocols. QRE does not require an external feedback with calculation since the Hamiltonian interactions are designed *a priori* to determine the final state avoiding uncertainty induced by the quantum-classical interface. In addition, QRE is less susceptible to experimental noise [19] and in some cases thrives in a noisy environment [20].

QRE has been demonstrated in macroscopic atomic ensembles [21], trapped atomic systems [22–24], and superconducting circuits [25–27]. Circuit quantum electrodynamics (CQED) systems are an attractive platform for QRE due to the experimental freedom to design strong interactions between superconducting qubits and microwave cavities [28]. Interactions between a superconducting transmon qubit and a microwave cavity have demonstrated qubit-photon entanglement [28] and the creation of quantum oscillator states [29,30]. Investigations using three dimensional waveguide cavities resulted in increased coherence times [31,32] in CQED structures allowing the observation of novel cavity quantum phenomena [33,34], yet no demonstration of a cavity photon-number state QRE protocol exists.

In this Letter, we demonstrate a new regime of CQED: the single-photon-resolved cross-Kerr effect [35] between two superconducting microwave cavities. This nonlinear coupling causes an excitation in one cavity to change the resonance frequency of the other cavity by more than their combined linewidth. While the state dependent shift between a qubit and a cavity has been previously shown [36,37], we present results for the first observation of a state dependent shift directly between two microwave cavities via a cross-Kerr effect [38]. In this Letter, a transmon is used to introduce nonlinearities to the cavities and for tomography. This new regime of CQED enables the first demonstration of a CQED QRE protocol that stabilizes quantum states of a microwave cavity. With this QRE protocol, we stabilize a primarily one-photon Fock state and show that its steady state Wigner function has negativity for all times. Furthermore, since the cavity is restricted to its first two energy levels, the stabilization can be described as a population inversion and as an effective negative temperature. This protocol could be extended to higher photon states of the microwave cavity by including more cw drives. The single-photon-resolved cross-Kerr interaction is necessary for a QRE protocol that stabilizes cat states of an oscillator [39] and may be used as a cavity-cavity entangling operation.

Within a CQED framework, we model our system as two harmonic oscillators coupled to a nonlinear oscillator. The most nonlinear oscillator in our circuit is the transmon whose nonlinearity originates from the Josephson junction with an inductance that is nonlinear with respect to the flux across it. This system is well described by the following Hamiltonian [40]:

$$\mathbf{H}/\hbar = \omega_q \mathbf{a}^\dagger \mathbf{a} + \omega_s \mathbf{b}^\dagger \mathbf{b} + \omega_c \mathbf{c}^\dagger \mathbf{c} - \frac{A_q}{2}\mathbf{a}^{\dagger 2}\mathbf{a}^2 - \frac{A_s}{2}\mathbf{b}^{\dagger 2}\mathbf{b}^2 - \frac{A_c}{2}\mathbf{c}^{\dagger 2}\mathbf{c}^2 - \chi_{qs}\mathbf{a}^\dagger \mathbf{a}\mathbf{b}^\dagger \mathbf{b} - \chi_{qc}\mathbf{a}^\dagger \mathbf{a}\mathbf{c}^\dagger \mathbf{c} - \chi_{sc}\mathbf{b}^\dagger \mathbf{b}\mathbf{c}^\dagger \mathbf{c}. \quad (1)$$

The subscripts used in the Hamiltonian are "q" for the transmon qubit, "s" for the storage cavity, and "c" for the cooling cavity. On the first line, ω_i denotes dressed angular frequencies. The second line contains self-interaction Kerr type terms of the modes, called anharmonicities, denoted by A_i. On the final line are the state dependent shifts χ_{ij} between modes. The state dependent shift to fourth order in junction flux is proportional to the geometric mean of the anharmonicities of the modes $\chi_{ij} \approx 2\sqrt{A_i A_j}$ [40], a strong, dispersive interaction between modes requires an appreciable anharmonicity for each mode [41].

To measure the storage cavity anharmonicity, we use a single cw drive to perform spectroscopy measuring the storage cavity frequency by looking at the transmitted signal through the low power peak of the cooling cavity [42], Fig. 1(a). Because of the large cross-Kerr interaction between the storage and cooling cavity, a tone on resonance with the storage cavity will change the frequency of the cooling cavity by more than a linewidth preventing transmission through the low power peak of the cooling cavity. Using a large amplitude drive, that power broadens the $f_{s,0\to1}$ ($f_i = \omega_i/2\pi$) transition, we observe the two-photon transition with frequency $f_{s,0\to2}/2$. The detuning corresponds to half the anharmonicity, A_s, of the storage cavity and we infer an inherited cavity anharmonicity $A_s/2\pi = 4.0$ MHz. Following the same method, we measure the cooling cavity anharmonicity as $A_c 2\pi = 300$ kHz when the cooling cavity linewidth is narrow (33 kHz). For the Fock state stabilization measurement, the cooling cavity linewidth is increased to 1.7 MHz and we measure its anharmonicity by having a calibrated drive corresponding to on average a single photon in the cooling cavity. By increasing the drive power applied to the cooling cavity and tracking the frequency shift we extract the same value for its anharmonicity.

To measure the state dependent shift between the two cavities, we first perform a 5 ns square pules which displaces the storage cavity state then perform a weak spectroscopic drive on the low power peak of the cooling cavity exciting the cooling cavity and finally apply a large amplitude drive at the high-power peak of the cooling cavity for the Jaynes-Cummings readout which relies on the inherited cooling cavity anharmonicity for discrimination in the readout signal [43]. Shown in Fig. 1(b) is a spectroscopy measurement of the cooling cavity for a storage cavity displacement corresponding to $\bar{n} \approx 1.5$ of the storage cavity. Discrete spectral peaks for up to three photons in the storage cavity are visible. From this, we infer a state dependent shift $\chi_{sc}/2\pi = 2.59 \pm 0.06$ MHz and observe the first single-photon-resolved cavity-cavity cross-Kerr interaction [44].

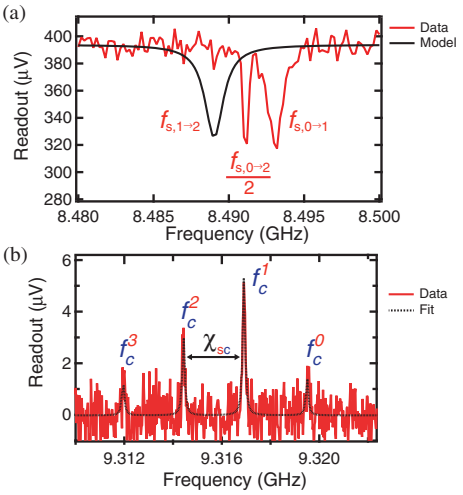

FIG. 1 (color online). Storage and cooling cavity spectra. (a) Spectroscopy is performed on the storage cavity with a single cw drive. With a large amplitude drive, we observe the two-photon transition $f_{s,0\to2}/2$. From this measurement we infer the location of the $f_{s,1\to2}$ transition (solid black line) and determine its detuning from the $f_{s,0\to1}$ transition as 4.0 MHz, which we define as the anharmonicity of the storage cavity. (b) A 5 ns square pulse, which displaces the storage cavity state and whose amplitude gives $\bar{n} \approx 1.5$ in the storage cavity, enables the observation of a single-photon-resolved cross-Kerr interaction between the two cavities, $\chi_{sc}/2\pi = 2.59 \pm 0.06$ MHz.

The measured Hamiltonian parameters lend themselves well to a CQED QRE protocol that stabilizes Fock states in a microwave cavity. The first requirement for the protocol shown in Fig. 2 is that the cavity in which Fock states will be stabilized is more anharmonic than its natural linewidth, $A_s > \kappa_s$, so that individual transitions may be selectively driven [Fig. 2(a), left]. A second requirement is a state dependent shift between the two cavities that is larger than both of their linewidths, $\chi_{sc} > \kappa_s, \kappa_c$ [Fig. 2(a), right]. In Fig. 1, we see that these requirements are met. However, this protocol is most successful when the lifetimes of the storage cavity and the cooling cavity are quite different $\kappa_c \gg \kappa_s$. In Fig. 1(b), the decay rates of the cavities are comparable, $(\kappa_c/\kappa_s \approx 4)$. We alter the ratio of lifetimes between the two cavities to a factor of 25 by increasing the cooling cavity coupling strength to the external environment.

Shown in Fig. 2(b) is a QRE protocol that stabilizes a one-photon Fock state in the storage cavity. This protocol is conceptually similar to the protocol used in Ref. [26], which stabilized the ground state of a qubit tensor product with a coherent state of a cavity. Although we stabilize the ground state of the storage cavity, we also use this protocol

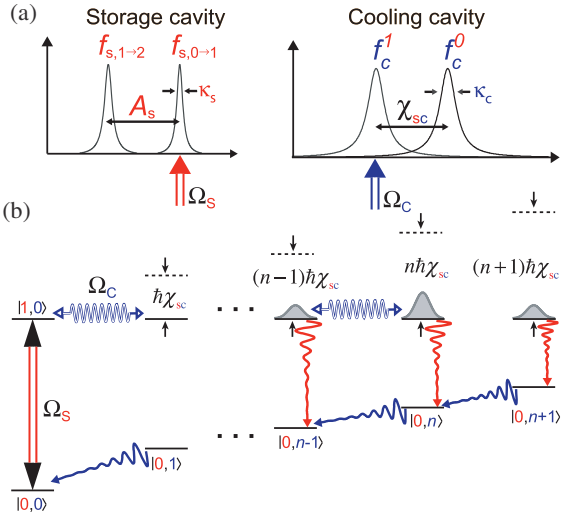

FIG. 2 (color online). Ideal cavity spectrum and Fock state stabilization protocol. (a) Left: sketch of idealized storage cavity spectrum. The storage cavity must have unequal energy levels spacing ($\hbar A_s$), inherited from the coupled qubit, to selectively drive storage cavity transitions. On the right is the idealized cooling cavity spectrum. The frequency shift of the cooling cavity due to photons in the storage cavity, the cross-Kerr effect (χ_{sc}), must be larger than either cavity linewidth to selectively drive this transition. (b) Energy level diagram for the coupled cavity-cavity system tracing over the qubit state. Excitations ascending vertically in the storage cavity while excitations ascend horizontally in the cooling cavity. A microwave drive Ω_S is applied on the storage cavity so that population only oscillates between vacuum and the first Fock state of the storage cavity. Simultaneously, a drive, Ω_C, is applied on the cooling cavity such that it is resonant provided there is exactly one excitation in the storage cavity. Once resonant, the cooling cavity is pumped to a mean photon-number set by the strength of the drive. Cavity decays, decaying arrows, close the autonomous loop of this protocol returning the population to $|0,0\rangle$ allowing the preparation to be repeated.

to stabilize a primarily one-photon Fock state. Because of the anharmonicity of the storage cavity, a cw drive (Ω_S) can be applied to the $f_{s,0\to1}$ transition. This drive is an induced Rabi rate on the storage cavity between vacuum and a one-photon Fock state. Concurrently with Ω_S, a drive with strength Ω_C is applied detuned by one cross-Kerr interaction from the cooling cavity. This drive is resonant provided that there is exactly one photon in the storage cavity. Once resonant, the conditional drive displaces the cooling cavity to a coherent state determined by the amplitude of the drive. When a photon decays from the storage cavity Ω_C, is no longer resonant and the cooling cavity quickly decays to vacuum. Once back to the ground state, the storage cavity is resonant with the drive Ω_S. This protocol reaches its steady state solution in a time governed by the decay rate of the cooling cavity. The steady state population in the one-photon Fock state of the storage cavity will be determined by its decay rate κ_s and the stabilization rate $\kappa_\uparrow$. The stabilization rate is defined as the rate at which the system is returned to the target state when a photon decays from the storage cavity. Using a simple four state model, we expect that to achieve a 99% one-photon Fock state in the storage cavity, a minimum ratio of lifetimes between the two cavities of 300 is required [45].

The Fock state stabilization protocol requires both the frequencies of the two microwave drives and their amplitudes be chosen appropriately. From a full simulation of the Linblad master equation as well as our experimental observations, we find optimal performance when $\Omega_S \approx \kappa_c$. We determine the drive power applied to the cooling cavity through a power dependent dephasing measurement of the transmon qubit applied roughly at one cross-Kerr interaction detuned from the cooling cavity.

The experimental implementation begins with cw drives applied simultaneously to the storage and cooling cavity for a duration of $200\kappa_c^{-1}$, which is twenty times longer than the time necessary to reach steady state [26] and roughly eight times longer than κ_s. To measure the photon population in the storage cavity, we stop the drives, wait for photons to decay from the cooling cavity, and apply conditional qubit π pulses to determine the photon number in the storage cavity [33,46].

We plot the steady state polarization $p = [P(0) - P(1)/P(0) + P(1)]$ of the storage cavity after running the protocol in Fig. 3(b). $P(n)$ corresponds to the probability of having exactly n photons in the storage cavity. Because of the selectivity of the drive Ω_S, the storage cavity is limited to its first two Fock states. We confirm this by measuring populations for the two- and three-photon Fock states and measure no statistically significant populations in these states. When Ω_C is driven at the zero-photon peak of the cooling cavity we observe $p = 0.95$ demonstrating that storage cavity is overwhelming in the zero-photon Fock state despite the induced Rabi drive on the storage cavity. However, as the drive power and frequency applied to the cooling cavity are varied, steady state stabilization of a polarization inversion occurs corresponding to a predominantly one-photon Fock state in the storage cavity. This population inversion is a purely quantum effect and can be described as an effective negative temperature according to

$$T = \frac{hf_{s,0\to1}}{2k_B \tanh^{-1}(p)}. \tag{2}$$

In Eq. (2), h is Planck's constant and k_B is Boltzmann's constant. From Eq. (2), when stabilizing a predominately $N = 1$ Fock state, the effective negative temperature of our quantum system is -0.77 ± 0.06 K.

In Fig. 3(d), plotted on top of the data is a full simulation of our driven dissipative system [47] where we find excellent agreement in our time dynamics. From the four state model, we would expect a polarization of $p = -0.47$. This value is within a factor of 2 of both what is measured experimentally and extracted from a full simulation of the Linblad equation. Through simulation of the full Linblad master equation we find that the limitation in polarization inversion is due to the finite ratio of lifetimes.

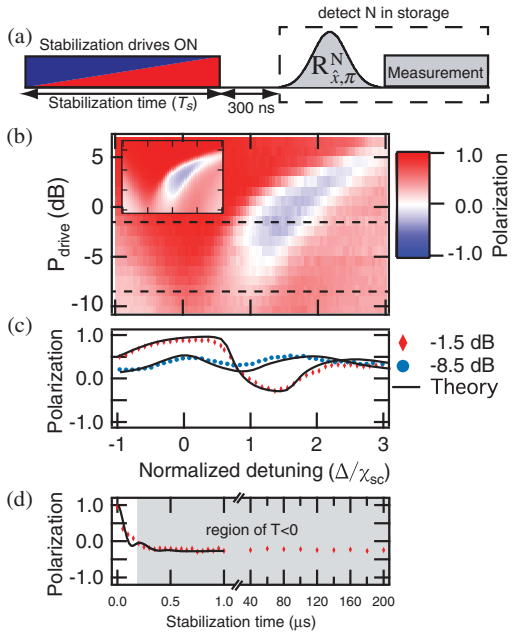

FIG. 3 (color online). Storage cavity polarization. (a) The Fock state stabilization protocol described in Fig. 2(b) is applied for a duration T_s, followed by a 300 ns wait to evacuate excitations from the cooling cavity, a photon selective π pulse is then performed on the qubit determining the probability of each photon state of the storage cavity up to three photons. (b) Storage cavity state polarization as a function of drive amplitude and frequency. The frequency of the cooling cavity drive is plotted as $\Delta = \omega_c^0 - \omega_{dc}$, and normalized by the cross-Kerr effect χ_{sc}. As the frequency of the drive applied to the cooling cavity is brought in resonance with the first photon peak of the storage cavity $\Delta/\chi_{sc} \approx 1$ the protocol stabilizes the first Fock state of the storage cavity. In simulation, we determine maximum polarization inversion corresponds to roughly four photons on average in the cooling cavity which explains why maximal stabilization occurs further detuned. The inset is a simulation plot with the same axis and color scale as the experimental result. (c) Line cuts for a weak drive power and a drive power resulting in a polarization inversion. (d) As the duration of the stabilization protocol is varied the polarization of the storage cavity alters and for infinite time reaches its steady state solution.

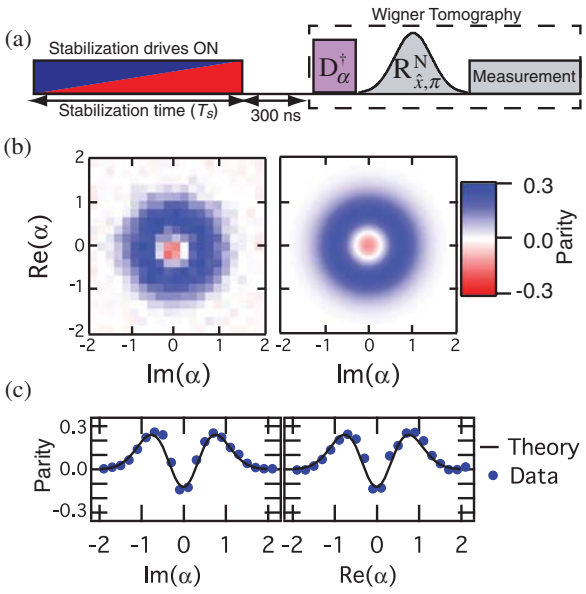

FIG. 4 (color online). Wigner tomography of stabilized steady state of the storage cavity. (a) The previously described stabilization protocol is used to reach the desired steady state. Then Wigner tomography is performed on the state of the storage cavity. (b) Left: Measured Wigner function for the steady state of the storage cavity which is a statistical mixture of an $N = 1$ and $N = 0$ Fock state. Right: Simulated steady state of the protocol. (c) Line cuts along $\mathrm{Im}(\alpha)$ and $\mathrm{Re}(\alpha)$ for the measured Wigner function and the simulated steady state Wigner function. Although not a pure $N = 1$ Fock state of the storage cavity our steady state solution does have negativity in the Wigner function indicative of a quantum state.

Although much of the discussion of the Fock state stabilization results has framed the storage cavity in the language of spin systems, it is still an oscillator. To demonstrate the oscillator nature of the storage cavity in Fig. 4, we perform cavity tomography measuring generalized Husimi Q functions, $Q_N(\alpha) = \pi^{-1}|\langle N|D_{-\alpha}|\Psi\rangle|^2$ [33], up to $N = 3$ Fock state of the storage cavity, $D_{-\alpha}$ is the displacement operator, and Ψ is the final state. We infer the Wigner function by adding and subtracting the even and odd measured Q functions. We compare these results to the Wigner function of a simulation of the steady state solution to the Fock state stabilization protocol [Figs. 4(b) and 4(c)]. Our results are explained in terms of a harmonic oscillator picture with the steady state of the storage cavity in a statistical mixture of $P(0) = 0.37 \pm 0.03$, $P(1) = 0.63 \pm 0.02$, and $P(2)$, $P(3)$ containing no statistically significant populations. In Fig. 4(c), negativity in the Wigner function is demonstrated for all times.

In conclusion, we present the first single-photon-resolved cross-Kerr effect between two cavities. We used the new regime of CQED to implement a CQED QRE protocol that stabilizes Fock states in a superconducting microwave cavity. We demonstrate one such instance, stabilizing a primarily $N = 1$ Fock state, quantified by the measured Wigner function of the storage cavity. This protocol can be extended to higher photon numbers of the storage cavity by including more selective microwave drives at the different transitions of the storage cavity. Our steady state polarization inversion corresponds to $p = -0.26 \pm 0.04$, which we map to the storage cavity being in equilibrium with a bath of $T = -0.77 \pm 0.06$ K. Our protocol is limited by induced spontaneous emission to the environment. Future implementations would benefit from a Purcell filter and increased nonlinearity in the CQED system.

This research was supported by the NSF under Grant No. PHY-1309996, the NSA through ARO Grants No. W911NF-09-1-514 and No. W911NF-14-1-0011, and the IARPA under ARO Contract No. W911NF-09-1-0369.

[1] M. A. Nielsen and I. L. Chuang, *Quantum Computation and Quantum Information* (Cambridge University Press, Cambridge, 2010).

[2] M. H. Devoret and R. J. Schoelkopf, Science **339**, 1169 (2013).

[3] A. R. Calderbank and P. W. Shor, Phys. Rev. A **54**, 1098 (1996).

[4] R. Laflamme, C. Miquel, J. P. Paz, and W. H. Zurek, Phys. Rev. Lett. **77**, 198 (1996).

[5] A. M. Steane, Phys. Rev. Lett. **78**, 2252 (1997).

[6] J. M. Geremia, Phys. Rev. Lett. **97**, 073601 (2006).

[7] C. Sayrin, I. Dotsenko, X. Zhou, B. Peaudecerf, T. Rybarczyk, S. Gleyzes, P. Rouchon, M. Mirrahimi, H. Amini, M. Brune *et al.*, Nature (London) **477**, 73 (2011).

[8] X. Zhou, I. Dotsenko, B. Peaudecerf, T. Rybarczyk, C. Sayrin, S. Gleyzes, J. M. Raimond, M. Brune, and S. Haroche, Phys. Rev. Lett. **108**, 243602 (2012).

[9] B. Peaudecerf, C. Sayrin, X. Zhou, T. Rybarczyk, S. Gleyzes, I. Dotsenko, J. M. Raimond, M. Brune, and S. Haroche, Phys. Rev. A **87**, 042320 (2013).

[10] S. Brakhane, W. Alt, T. Kampschulte, M. Martinez-Dorantes, R. Reimann, S. Yoon, A. Widera, and D. Meschede, Phys. Rev. Lett. **109**, 173601 (2012).

[11] M. Blok, C. Bonato, M. Markham, D. Twitchen, V. Dobrovitski, and R. Hanson, Nat. Phys. **10**, 189 (2014).

[12] D. Ristè, C. C. Bultink, K. W. Lehnert, and L. DiCarlo, Phys. Rev. Lett. **109**, 240502 (2012).

[13] D. Ristè, M. Dukalski, C. A. Watson, G. de Lange, M. J. Tiggelman, Y. M. Blanter, K. W. Lehnert, R. N. Schouten, and L. DiCarlo, Nature (London) **502**, 350 (2013).

[14] D. Riste, S. Poletto, M. Z. Huang, A. Bruno, V. Vesterinen, O. P. Saira, and L. DiCarlo, Nat. Commun. **6**, 6983 (2015).

[15] J. F. Poyatos, J. I. Cirac, and P. Zoller, Phys. Rev. Lett. **77**, 4728 (1996).

[16] S. Diehl, A. Micheli, A. Kantian, B. Kraus, H. Büchler, and P. Zoller, Nat. Phys. **4**, 878 (2008).

[17] B. Kraus, H. P. Büchler, S. Diehl, A. Kantian, A. Micheli, and P. Zoller, Phys. Rev. A **78**, 042307 (2008).

[18] C. A. Muschik, E. S. Polzik, and J. I. Cirac, Phys. Rev. A **83**, 052312 (2011).

[19] C. A. Muschik, H. Krauter, K. Jensen, J. M. Petersen, J. I. Cirac, and E. S. Polzik, J. Phys. B **45**, 124021 (2012).

[20] K. G. H. Vollbrecht, C. A. Muschik, and J. I. Cirac, Phys. Rev. Lett. **107**, 120502 (2011).

[21] H. Krauter, C. A. Muschik, K. Jensen, W. Wasilewski, J. M. Petersen, J. I. Cirac, and E. S. Polzik, Phys. Rev. Lett. **107**, 080503 (2011).

[22] J. T. Barreiro, M. Müller, P. Schindler, D. Nigg, T. Monz, M. Chwalla, M. Hennrich, C. F. Roos, P. Zoller, and R. Blatt, Nature (London) **470**, 486 (2011).

[23] Y. Lin, J. P. Gaebler, F. Reiter, T. R. Tan, R. Bowler, A. S. Sørensen, D. Leibfried, and D. J. Wineland, Nature (London) **504**, 415 (2013).

[24] D. Kienzler, H.-Y. Lo, B. Keitch, L. de Clercq, F. Leupold, F. Lindenfelser, M. Marinelli, V. Negnevitsky, and J. P. Home, Science **347**, 53 (2015).

[25] K. W. Murch, U. Vool, D. Zhou, S. J. Weber, S. M. Girvin, and I. Siddiqi, Phys. Rev. Lett. **109**, 183602 (2012).

[26] K. Geerlings, Z. Leghtas, I. M. Pop, S. Shankar, L. Frunzio, R. J. Schoelkopf, M. Mirrahimi, and M. H. Devoret, Phys. Rev. Lett. **110**, 120501 (2013).

[27] S. Shankar, M. Hatridge, Z. Leghtas, K. Sliwa, A. Narla, U. Vool, S. M. Girvin, L. Frunzio, M. Mirrahimi, and M. H. Devoret, Nature (London) **504**, 419 (2013).

[28] A. Wallraff, D. I. Schuster, A. Blais, L. Frunzio, R.-S. Huang, J. Majer, S. Kumar, S. M. Girvin, and R. J. Schoelkopf, Nature (London) **431**, 162 (2004).

[29] M. Hofheinz, E. M. Weig, M. Ansmann, R. C. Bialczak, E. Lucero, M. Neeley, A. D. O'connell, H. Wang, J. M. Martinis, and A. N. Cleland, Nature (London) **454**, 310 (2008).

[30] M. Hofheinz, H. Wang, M. Ansmann, R. C. Bialczak, E. Lucero, M. Neeley, A. D. O'Connell, D. Sank, J. Wenner, J. M. Martinis *et al.*, Nature (London) **459**, 546 (2009).

[31] H. Paik, D. I. Schuster, L. S. Bishop, G. Kirchmair, G. Catelani, A. P. Sears, B. R. Johnson, M. J. Reagor, L. Frunzio, L. I. Glazman *et al.*, Phys. Rev. Lett. **107**, 240501 (2011).

[32] M. J. Reagor, H. Paik, G. Catelani, L. Sun, C. Axline, E. T. Holland, I. M. Pop, N. A. Masluk, T. Brecht, L. Frunzio *et al.*, Appl. Phys. Lett. **102**, 192604 (2013).

[33] G. Kirchmair, B. Vlastakis, Z. Leghtas, S. E. Nigg, H. Paik, E. Ginossar, M. Mirrahimi, L. Frunzio, S. M. Girvin, and R. J. Schoelkopf, Nature (London) **495**, 205 (2013).

[34] Z. Leghtas, S. Touzard, I. M. Pop, A. Kou, B. Vlastakis, A. Petrenko, K. M. Sliwa, A. Narla, S. Shankar, M. J. Hatridge, M. Reagor, L. Frunzio, R. J. Schoelkopf, M. Mirrahimi, and M. H. Devoret, Science **347**, 853 (2015).

[35] Y. Hu, G.-Q. Ge, S. Chen, X.-F. Yang, and Y.-L. Chen, Phys. Rev. A **84**, 012329 (2011).

[36] P. Bertet, A. Auffeves, P. Maioli, S. Osnaghi, T. Meunier, M. Brune, J.-M. Raimond, and S. Haroche, Phys. Rev. Lett. **89**, 200402 (2002).

[37] D. I. Schuster, A. A. Houck, J. A. Schreier, A. Wallraff, J. M. Gambetta, A. Blais, L. Frunzio, J. Majer, B. R. Johnson, M. H. Devoret *et al.*, Nature (London) **445**, 515 (2007).

[38] B. Fan, A. F. Kockum, J. Combes, G. Johansson, I.-c. Hoi, C. M. Wilson, P. Delsing, G. J. Milburn, and T. M. Stace, Phys. Rev. Lett. **110**, 053601 (2013).

[39] A. Roy, Z. Leghtas, A. D. Stone, M. H. Devoret, and M. Mirrahimi, Phys. Rev. A **91**, 013810 (2015).

[40] S. E. Nigg, H. Paik, B. Vlastakis, G. Kirchmair, S. Shankar, L. Frunzio, M. H. Devoret, R. J. Schoelkopf, and S. M. Girvin, Phys. Rev. Lett. **108**, 240502 (2012).

[41] See Supplemental Material at http://link.aps.org/supplemental/10.1103/PhysRevLett.115.180501 for a photo of the experimental setup.

[42] D. I. Schuster, A. Wallraff, A. Blais, L. Frunzio, R.-S. Huang, J. Majer, S. M. Girvin, and R. J. Schoelkopf, Phys. Rev. Lett. **94**, 123602 (2005).

[43] M. D. Reed, L. DiCarlo, B. R. Johnson, L. Sun, D. I. Schuster, L. Frunzio, and R. J. Schoelkopf, Phys. Rev. Lett. **105**, 173601 (2010).

[44] See Supplemental Material at http://link.aps.org/supplemental/10.1103/PhysRevLett.115.180501 for a table of all Hamiltonian parameters in Eq. (1).

[45] See Supplemental Material at http://link.aps.org/supplemental/10.1103/PhysRevLett.115.180501 for a derivation of the four state model.

[46] B. Vlastakis, G. Kirchmair, Z. Leghtas, S. E. Nigg, L. Frunzio, S. M. Girvin, M. Mirrahimi, M. H. Devoret, and R. J. Schoelkopf, Science **342**, 607 (2013).

[47] J. Johansson, P. Nation, and F. Nori, Comput. Phys. Commun. **184**, 1234 (2013).